Development of chitosan/starch films reinforced with ZnO nanostructures from waste batteries

C. López-Díaz de León[1], I. Olivas-Armendáriz[1*], E. Duarte-Fierro[1], E. Flores-Gerardo[1], J. F. Hernandez-Paz[1], M. Hernández-González[2], M. C. Chavarría-Gaytán[1], C. A. Rodríguez-González[1]

[1]*Instituto de Ingeniería y Tecnología, Universidad Autónoma de Ciudad Juárez, Ave. Del Charro #610 norte, Col. Partido Romero, C.P.32320, Cd. Juárez, Chihuahua, México.*
[2] *Universidad Autónoma Agraria Antonio Narro, Calzada Antonio Narro 1923, Buenavista, Saltillo Coahuila, 25315, México.*

Abstract
Large amounts of materials end their life cycle in places where no re-use or recycling is considered to extend their life, thus causing unnecessary contamination that in time can cause severe damage to the environment and the population health. To improve the life cycle of waste batteries, ZnO nanoparticles were obtained by an environmentally friendly sol-gel process from the battery anode and used to manufacture biodegradable chitosan/starch films containing 1, 3, 5, and 7% of ZnO nanoparticles. The incorporation of ZnO nanoparticles to the chitosan/starch films resulted in higher tensile strength and elongation at break, the water resistance increased considerably, and their antimicrobial properties increased as compared to neat chitosan/starch films. Maximum antibacterial activity against *S. aureus* inoculated during refrigerated storage was obtained with films containing 7% ZnO nanoparticles. FTIR spectra and DMA revealed intermolecular interactions between the polymer matrix and the ZnO nanoparticles. The results indicate a good premise in terms of tailoring films with ZnO nanoparticles obtained from waste batteries that could determine or enhance the properties of the films composite materials.

1. Introduction

There are currently large amounts of material that ends its life time, and there is no continuity in its life cycle to avoid the waste generation and allow its re-use as part of other products. This has an impact on the generation of material that it is commonly called garbage and environmentally represents a hazard, due to the latent contamination that can generate around it. This situation has led to research into the life cycle of different materials and their reuse through their incorporation into other processes [1, 2] and the development of materials that can be used in specific applications such as biodegradable polymeric films.

Among the biopolymers used in the manufacture of films are polysaccharides such as chitosan and starch which are widely available because they come from renewable and low-cost sources [3, 4]. Chitosan is an antimicrobial, biodegradable, biocompatible and with unique biofunctional properties [5] making it a suitable candidate to substitute synthetic materials as a mean to reduce negative impacts on the environment when used in the manufacture of active films. On the other hand, starch has been used in

the manufacture of biodegradable films [6]. It has been demonstrated that starch-based films have good homogeneity, flexibility, transparency, and rapid biodegradability [7]. In addition to reduce moisture loss, restrict oxygen absorption, decrease the migration of fats, present total composability without generating any hazardous residues, control flavor transfer components to increase shelf life and prevent deterioration of the quality of food products and enable its applications in tissue engineering [3, 8].

In recent years the demand for nanomaterials such as zinc oxide (ZnO) obtained from waste batteries has increased, through environmentally friendly synthesis methods such as sol-gel process. ZnO nanoparticles have been incorporated into different polymers films for packaging in order to improve their mechanical [9], barrier [10], antibacterial [11] and wettability [9] properties as well as their ability to block UV radiation. Also, ZnO has been generally classified as a secure material (GRAS) by the U. S. Food and Drug Administration [12].

Disposal of waste batteries represents an environmental problem of heavy metals since they are discarded without any suitable regulation. Therefore, batteries are considered as a secondary source of raw material, since valuable metals such as zinc, manganese, and steel can be recovered and put on the market for the manufacture of batteries or other products. There are different batteries recycling processes, considering the hydrometallurgical extraction method, a more friendly process to the environment because the used reagents are less dangerous, and the generated waste is minimal. This method consists of different pretreatment steps, followed by leaching out and separation of metals by electrolysis, extraction, or precipitation [13].

This research aimed at the development and characterization of polymeric films based on chitosan and starch, reinforced with zinc oxide nanoparticles obtained from waste alkaline batteries.

2. Material and Methods

2.1. Synthesis of ZnO nanoparticles by sol-gel method

Waste type D alkaline batteries were used as a source of zinc for the synthesis of the nanoparticles, using the methodology previously used by our team [10].

2.2. Synthesis of chitosan/starch films reinforced with ZnO nanoparticles

1.4 g of chitosan (medium molecular weight Aldrich 448877) were dissolved in 60 mL of 1% acetic acid solution (Sigma-Aldrich 99.7% 695092), 0.6 g of rice starch were dissolved (Sigma-Aldrich S7260) in 30 mL of distilled water adding 1 mL of 70% sorbitol aqueous solution (Golden Bell 54280), to improve the flexibility of the film 1 mL of glycerol was added (99% AlfaAesar 16205). Both solutions (chitosan and starch) were then mixed under constant agitation and the ZnO nanoparticles added in proportions of 1, 3, 5, and 7% (weight). The chitosan/starch films were named for the content of nanoparticles in their composition, and a control film was preserved (chitosan/starch films without nanoparticles). Finally, the mixtures were sonicated for 5 min (0.5 Cycle 100 % Amplitude) for particle homogenization and then deposited in Petri dishes and left to dry for 48 hours.

2.3. Characterization of chitosan/starch films reinforced with ZnO nanoparticles

2.3.1 Field emission scanning electron microscopy (FESEM) and X-ray energy dispersion spectroscopy (EDS)

FESEM images were obtained with a Jeol JSM7000F. The electron beam accelerating voltage was 15 kV (low vacuum mode). The particle size was measured using the Image J program. EDS was performed using the Oxford X-act Penta FET Precision accessory.

2.3.2 Fourier transform infrared spectrometry (FTIR)

The films were cut and mounted on an ATR adapter with Germanium crystal for analysis (Nicolet 6700). All spectra were recorded using 100 scans and 16 cm^{-1} resolution. All the samples were scanned within the range 550–4000 cm^{-1}.

2.3.3 Dynamic-mechanical analysis (DMA)

Dynamic mechanical analysis was made using a DMA2890 TA Instrument, using a heating rate of 5°C per minute, a frequency of 1Hz, running a temperature ramp from room temperature to 35°C. Analysis performed with samples of 8 cm x 2 cm. The test was performed according to ASTM D412 standard, modifying the test speed and sample size.

2.3.4 Determination of the contact angle

The hydrophilic nature of the films was evaluated measuring the contact angle by depositing a drop of distilled water on the surface of each sample at room temperature, using a goniometer (KRUSS, DSA30). Three repetitions were made for each film in the analysis.

2.3.5 Water vapor permeability (WVP)

Water vapor permeability was determined through the methodology established by ASTM E96-05 (ASTM, 2005). Permeability cells, containing a hygroscopic agent, covered with the tested film face up, were storage in a climatic chamber at 100% Relative Humidity (RH) at room temperature.

Samples weight was measured every hour within 9 h. 3 repetitions for each formulation were evaluated in order to determine the water vapor permeability rates, according to the slope obtained through the weight gaining data linear regression according to the time exposure. WVP was calculated according to the following equation:

$$WVP = (Slope)(L)(24)/(A)(VP) \tag{1}$$

2.3.6 Biodegradability

Samples (2 cm x 8 cm) were placed in a phosphate buffer solution (PBS) (pH 7.4) containing 0.02% sodium azide (≥99%, ultra-dry, Sigma-Aldrich) and 5 µg/mL lysozyme enzyme (protein ≥90 %, Sigma-Aldrich). They were incubated at 37°C for different periods. Once the samples were removed from the PBS solution, they were repeatedly washed with deionized water. The degradation of the samples was evaluated in terms of weight loss, thickness change, pH variation, surface morphology, and modification of mechanical behavior. The mechanical properties at room temperature of the films were evaluated in a universal traction machine (Tinius Olsen, HSOKS) and tested at a speed of 5 mm/min, 500 N loading cell; three repetitions of each condition were performed. The surface morphology of the films was observed using SEM (Jeol JSM-7000F). FTIR spectra were obtained in a Nicolet 6700. The weight loss rate of the films was calculated according to Eq. (2).

$$q=(Wt-Wo)/Wo \ (100\%) \tag{2}$$

2.3.7 Cytotoxicity

Each film and negative control (only cells) was seeded with 5000 cells (3T3, ATCC®) immersed and incubated in DMEM supplemented with fetal bovine serum and antibiotic at 37°C. The films were extracted the medium in which they were during incubation, washed with PBS and added 200 µL of Dulbecco's Modified Eagle Medium (D-MEM, Invitrogen) solution containing 10% Fetal Bovine Serum

(FBS, GIBCO) and 1% antibiotic and 50 μL of MTT (5 mg/ml in phosphate buffered saline, PBS, 1X). Subsequently, they were incubated at 37°C for one hour. Next, the supernatant was removed, and 250μL of DMSO (dimethyl sulfoxide, Sigma-Aldrich) was added to each sample, to dissolve the formazan crystals. The absorbance was measured with a wavelength of 570 nm in a microplate reader (Benchmark Plus).

2.3.8 Evaluation of antimicrobial activity
The antimicrobial activity evaluation was performed using a Staphylococcus aureus (S. aureus) strain. It was supplied from the food safety laboratory of the Universidad Autónoma Agraria Antonio Narro. An infectious inoculum equivalent to tube four on the McFarland scale (1.2*109UFC/ml) was prepared in TSB broth. The pieces of ham were inoculated with the infectious preparation and coated with the films, placed in plastic bags and stored at refrigeration temperature. The counting of S. aureus of the coated ham and the control (pieces of ham not covered with the films) was performed at 12, 24, 36, 48, 60 and 96 h on Brain Heart Infusion (BHI) agar plates.
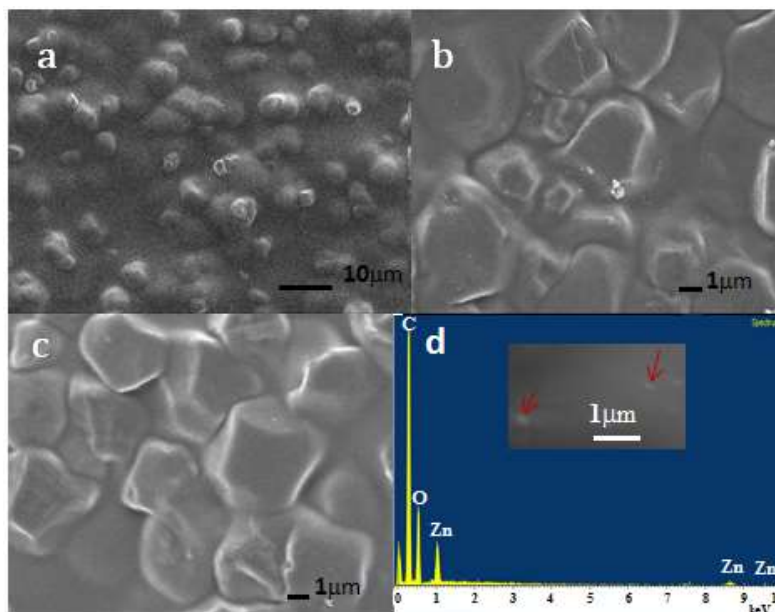
2.3.9 Statistic analysis
The results were evaluated of using variance analysis (ANOVA) and the Tukey test at a significance level of 5% using Statistica 12.0 software (StatSoft, Inc., Tulsa, USA). Data were presented as mean ± standard deviation.
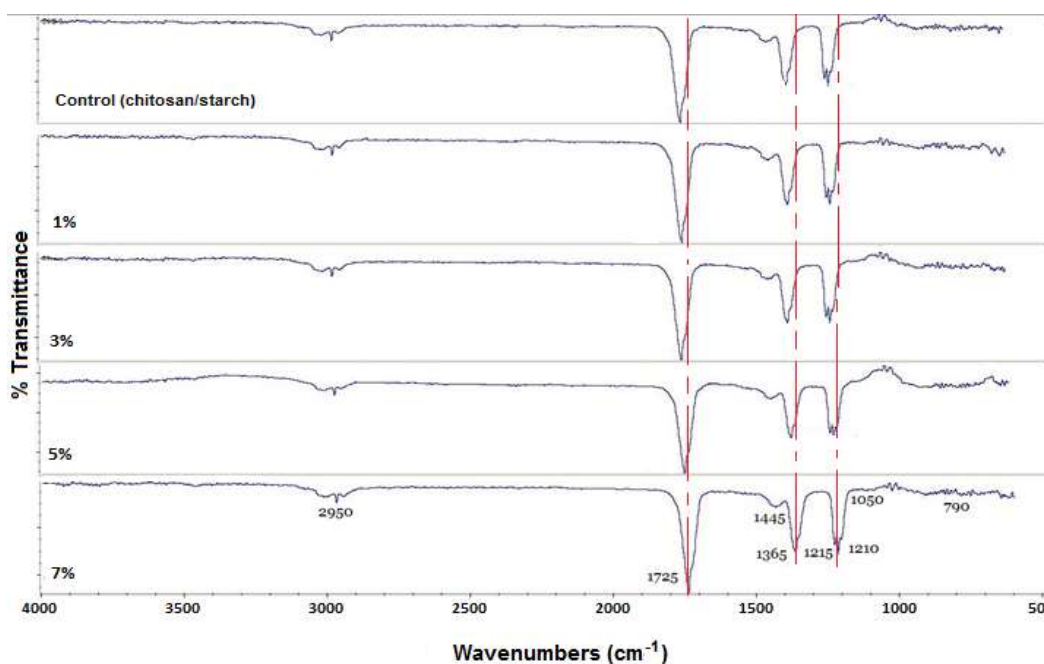
3. Results and discussion

Figure 1 (a, b, and c) shows SEM images of the films containing different percentages of nanoparticles. Nanoparticles are embedded throughout the polymer matrix. The topography of the surface is irregular and the presence of nanoparticles agglomerates (Figure 1-d) are observed at high magnification using low voltage (1KeV) for the analysis. Figure 1(d) also shows the EDS of the chitosan/starch film containing 3% zinc oxide nanoparticles. It shows the elementary composition of the films; zinc (Zn) that comes from the zinc oxide (ZnO) nanoparticles, oxygen (O) that can come from the ZnO nanoparticles or from the organic compounds and carbon (C) from the organic compounds of chitosan and starch. No impurities were found which is in agreement with our previous report for the ZnO nanoparticles obtained from wasted alkaline anodes [10].

Figure 2 shows the infrared spectra of the chitosan/starch films containing 0 (control film), 1, 3, 5, and 7% of zinc oxide nanoparticles. Spectra exhibit the typical signals of starch and chitosan, such as the bands assigned to the stretches of the CH_2 and CH_3 groups at 3000 and 2920 cm^{-1}, respectively. On the other hand, at 1725 cm^{-1}, the band attributed to stretching of the amide I is seen. As the content of nanoparticles is increased, a displacement towards lower wavenumbers is detected. This displacement has been associated with the change in the orientation and conformation of the polymer chains by the incorporation of zinc oxide nanoparticles [11]. Also, bands observed at 1445 and 1320 cm^{-1} are related to stretching of the N-H and tertiary amine, respectively [14]. On the other hand, the bands corresponding to an asymmetric stretching of the functional group C-O-C, the vibrations of the C-O group, and the flexion of the C-H group are observed at 1050, 1100, and 780 cm^{-1} [15]. When the content of ZnO nanoparticles in the chitosan/starch films increases small changes in the position of the bands on the N-H group and tertiary amine are seen, and it suggested that the ZnO nanoparticles interacted, via hydrogen bonding, with N-H groups. The effect of the ZnO nanoparticles on the mechanical properties of the films was studied by DMA. Figure 3 shows the structural changes in the mechanical properties of the control film and the films containing 1, 3, 5, and 7% of zinc oxide nanoparticles. The film containing 7% of

nanoparticles exhibited a higher storage modulus than the control film and those containing 1, 3, and 5% of nanoparticles (Fig. 3a); according to other researchers, it is attributed to the fact that the increasing concentration of nanoparticles results in closer and more rigid molecular chains.

Figure 1. SEM images and EDS of the chitosan/starch films with zinc oxide nanoparticles. Containing: a) 1, b) 3, c) 7, and d) 3% of zinc oxide nanoparticles.
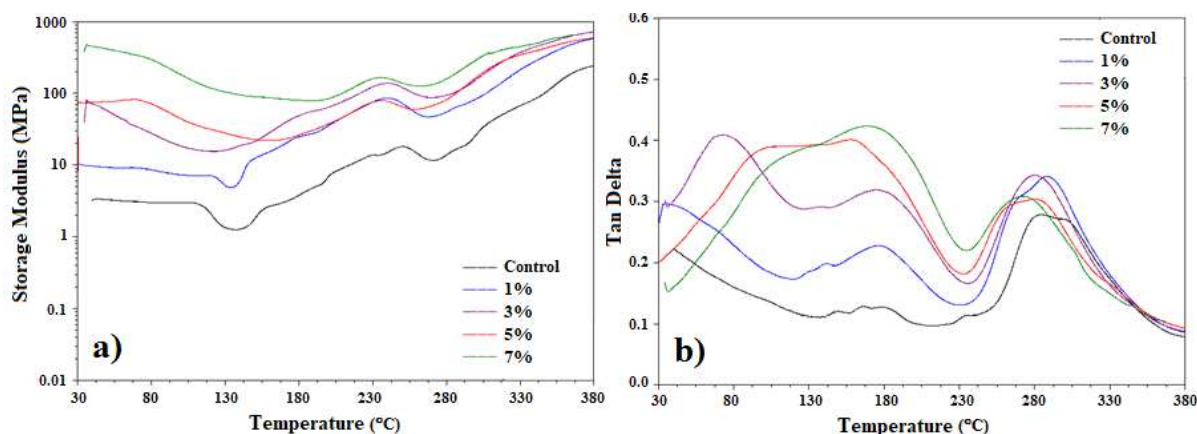

Figure 2. Infrared spectra of the chitosan/starch films containing 0, 1, 3, 5, and 7% zinc oxide nanoparticles.

The storage modulus is an index of the rigidity of polysaccharides [16]. On the other hand, the tan δ provided the glass transition temperature (Tg) of the films (Fig. 3b). The curves showed two peaks around 150-180°C and 260-290°C attributed to β and α chitosan relaxations, respectively. Results found in the case of chitosan/starch blend films [17]. Relating β relaxation with groups attached to the C-2 position in the main chain of chitosan and α relaxation with the glass transition of the amorphous phase [5, 16]. The change of the β and α transitions at higher temperatures is the result of the addition of ZnO

nanoparticles. These results could confirm those obtained by FTIR analysis; as may be due to an interaction between the polymer matrix and ZnO nanoparticles, however, it could also be induced by the effect of intermolecular effects.

Figure 3. a) Storage modulus and b) Tan delta as a function of the temperature of the dynamic mechanical analysis of the control, 1%, 3%, 5%, and 7% films.
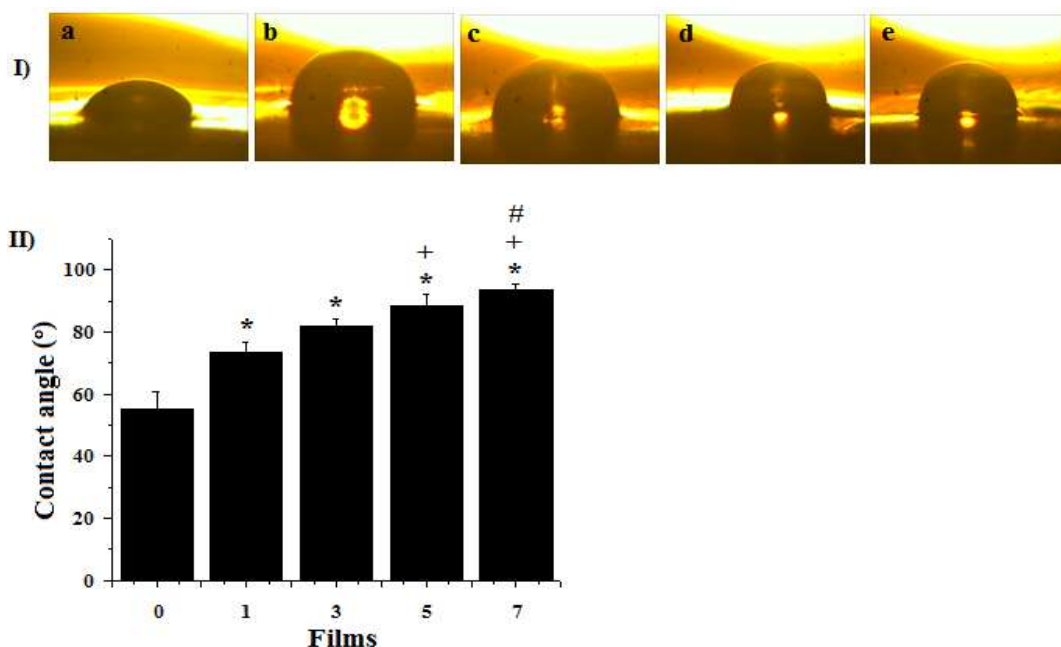
Mechanical tests were performed on films with thickness ranging from 136µm to 151µm (Table 1). All the chitosan/starch films reinforced with ZnO nanoparticles showed improved mechanical properties than the control films. The tensile strength and elongation at break gradually increased as the concentration of ZnO nanoparticles increased. The tensile strength significantly increased concerning the control film (10.89±0.00 MPa) by 1.48, 1.83, 1.87, and 2.45 times for the 1, 3, 5, and 7% films, respectively. The maximum value of 26.76±0.001 MPa was reached when the films were reinforced with 7% of nanoparticles. Increments that result in the tensile strength required for materials to be used as packing material (13-28 MPa) [18]. While the elongation at break exhibited a smaller effect than it did on tensile strength once the films obtained increases with respect to the control film (9.09%) by 1.11, 1.29, 1.73, and 2.08 times for the films 1, 3, 5, and 7%. These results can be attributed to the fact that the nanoparticles are homogeneously distributed through the polymer matrix, improving the brittleness of the chitosan/starch matrix due to the high stiffness of nanoparticles [9]. However, the mechanical properties, according to Niu, can not only be affected by the dispersion of nanoparticles in the matrix but also the interaction between the nanoparticles and the matrix and the volume fraction of the reinforcement.

Table 1. Thickness, tensile strength, and elongation at break of the films.

Film/ Tensile properties	Tensile strength (MPa)	Elongation at break (%)	Thickness (µm)
Control	10.89±0.00	9.09±0.35	136.12±1.94
1%	16.12±0.01	10.14±0.14	135.85±0.26
3%	19.94±0.00	11.73±0.76	139.20±4.53
5%	20.47±0.003	15.79±0.22	147.40±2.09
7%	26.76±0.001	18.91±0.37	151.02±5.66

The measured mean values of water contact angle on the surface of the polymer films containing ZnO nanoparticles are shown in Figure 4. An increase in the contact angle values of the chitosan/starch films occurred as the content of ZnO nanoparticles was increased, contact angles of 56, 74, 83, 88, and 94° for films containing 0, 1, 3, 5, and 7% of nanoparticles, respectively (Figure 4II). The results indicate

lower wettability in the films with nanoparticles concerning the control film. Saral and collaborators by adding 1 and 5% of ZnO nanoparticles to polyurethane/chitosan films obtained contact angles of 77 and 92.2°, similar results to those found in this investigation [19]. This could be due to the intermolecular interactions between the polymeric matrix and nanoparticles and the fact that the nanoparticles blocked the pores of the films and the increase in the roughness of the surface as the number of nanoparticles in the films increased, preventing the penetration and displacement of the drops of water.

Figure 4. I) Contact angles on surfaces and II) average water contact angles (°) of chitosan/starch films containing different percentages of ZnO nanoparticles: a) control, b) 1, c) 3, d) 5, and e) 7% of nanoparticles.

The Table 2 exposes the WVP data obtained for each formulation. (Data are presented as the means of the results obtained of the analysis in triplicate). It is possible to observe that there are not significant differences between WVP values for the 1, 3, and 5% films, which values range from $8.19*10^{-9}$ to $6.83*10^{-9}$ g*m/m^2*min*mm Hg. A slight lower difference was observed for the control film, which is $1.11*10^{-8}$ g*m/m^2*min*mm Hg. Reduction that may be due to the good dispersion of the nanoparticles in the polymer matrix and the decrease of wettability due to intermolecular interactions between the polymeric matrix and nanoparticles. Having more difficulty water molecules to pass through the film, since the nanoparticles act as an impermeable barrier in the diffusion process (great resistance to gas transport) [9]. These values are similar to those reported for commercial packing material such as LDPE ($6.94*10^{-9}$ g*m/m^2*min*mm Hg) and wax paper ($1.11*10^{-9}$ g*m/m^2*min*mm Hg) and much lower than the values reported for films obtained from starch by itself, $2.03*10^{-5}$ g*m/m^2*min*mm Hg. It is observed that the permeability does not change for the two films with 3 and 5% of ZnO nanoparticles content. Attributed, according to Marra and collaborators, to two opposing contributions (from the nanoparticles) such as: the impermeable barrier in the diffusion process and it is generated more free volume at the interfaces between nanoparticles and polymeric matrix [9]. Promising results since water could have a great effect on microbial development, influencing the shelf life of the packaged product. Figure 5I shows the weight loss, and Figure 5II the films surface morphology when exposed to PBS containing lysozyme in different periods. The films showed rapid biodegradation during the first week, 27.33, 26.48, 20.66, and 27.77 % for films containing 1, 3, 5, and 7% nanoparticles and 21.16% for control. During the second and third week, weight loss was maintained and reach near 30% except for

the film containing 7% of ZnO nanoparticles. At the end of 4 weeks, the weight loss of the films was 30.82, 30.31, 29.65, 29.65, and 24.82 % for control, 1, 3, 5, and 7% films. On the other hand, the FESEM images of the chitosan and starch films containing 0 and 7% of zinc oxide nanoparticles (Fig. 5II) show that the film that does not contain nanoparticles has a more extensive damaged area similar to a sponge (Fig. 5IId) than that presented by the film containing 7% of nanoparticles (Fig. 5IIh).

Table 2. Water Vapour Permeability.

Films	Permeability
	g*m/m^2*min*mm Hg
Control	1.11*10^{-8}
1%	8.19*10^{-9}
3%	6.83*10^{-9}
5%	6.83*10^{-9}

Results that could be attributed to the process of hydrolysis throughout the films. According to Yew and collaborators [20] spongy morphology is defined as the presence of medium-sized holes and individual holes leaving the granules. Surface attack is indicative of the enzymatic action through total damage to the surface or sections of the surface of the starch granule, which can facilitate the penetration and attack of the enzyme through greater water absorption of the polymer matrix of chitosan. This process is carried out by hydrolyzing α (1-4) and β (1-4) glycosidic bonds of the starch and chitosan by the enzyme which leads to a significant increase in the percentage of mass loss. This is confirmed by Araújo and his team, who mention that weight loss of polysaccharides (such as starch) of up to 20% may be because the enzyme increases the release of substrates of long-chain oligosaccharides, this being an evidence of the degradation of the material. Table 3 shows the tensile properties of the films after exposure to the enzyme solution. When comparing the tensile properties of the films exposed for 4 weeks to the enzymatic solution, it can be seen how they decrease as the exposure time increases. This indicates that the enzymatic solution influences these properties.
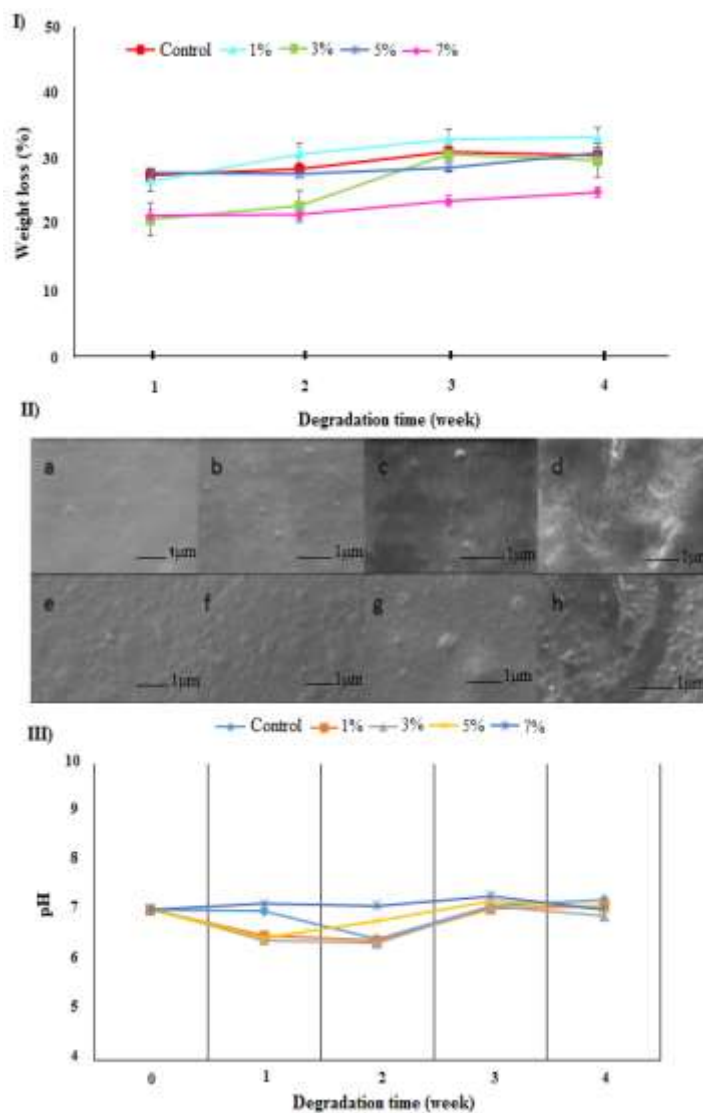
Table 3. Tensile properties and elongation at break of the films after exposure to the solution.

Films	Tensile properties/Time (week)	1	2	3	4
Control	Tensile strength (MPa)	11.03±0.58	3.30±0.17	1.939±0.01	1.32±0.00
	Elongation at break (%)	7.81±0.31	5.36±0.72	4.46±0.06	3.48±0.01
1%	Tensile strength (MPa)	6.52±0.20	4.89±0.45	3.32±0.16	1.49±0.00
	Elongation at break (%)	8.71±0.16	6.89±0.21	4.10±0.24	7.13±0.32
3%	Tensile strength (MPa)	9.82±0.05	3.92±0.11	3.746±0.01	1.76±0.00
	Elongation at break (%)	9.13±0.23	8.91±1.24	6.24±0.002	5.35±0.05
5%	Tensile strength (MPa)	10.61±1.25	4.05±0.42	3.129±0.56	4.40±0.04
	Elongation at break (%)	14.26±1.48	13.67±1.6	12.58±3.27	11.73±1.51
7%	Tensile strength (MPa)	20.01±2.3	14.15±2.11	6.347±0.001	3.25±0.17
	Elongation at break (%)	17.56±1.8	16.35±2.35	15.34±1.38	15.79±2.45

Confirming the observed in the FESEM and weight loss, the elimination of particles of starch from the surface of the material causes the formation of holes and damages in the form of a sponge which will lead to the decrease of the tensile properties. This can be attributed to water absorption by the polymer matrix of chitosan facilitating penetration of the enzyme into films, improving the attack of the same to the matrix of chitosan and starch, which confirms that the material is susceptible to treatment with the
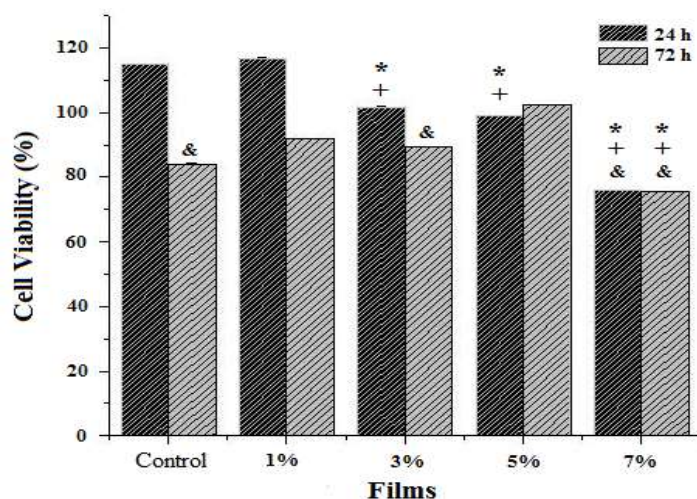
enzymatic solution [20]. Figure 5III shows the pH change of the solution containing the films during the study period. The degradation products had no influence on it, which remained close to 7.4 during the different periods. The results of the analysis of degradation showed biodegradable films, which observed weight loss between 25 and 31% during the study period, since they exhibit a hydrophilic character. It could be expected that when in contact with natural environments, once their function is fulfilled, its speed of biodegradation increases due to a greater absorption of water that promotes the growth of microorganisms present in the soil and that act on carbohydrates [21].

Fig. 5. I) Weight loss of the films in different periods of the enzymatic degradation. II) SEM images of enzymatic degradation analysis of chitosan/starch films containing 0 (control) and 7% of zinc oxide nanoparticles. a) Control, week 1; b) Control, week 2; c) Control, week 3; d) Control, week 4; e) 7%, week 1; f) 7%, week 2; g) 7%, week 3, and h) 7% week 4. III) The behavior of the pH of the solution during the study period.

The results of the cell viability of the fibroblasts exposed to the films are shown in Figure 6. It can be observed that, at the 24 h evaluation period, the control film and those containing 1, and 3% of nanoparticles presented a cell viability greater than 100%, being an adequate indication of the response of the cells to the material [4] with the exception of the 7% film that showed a cell viability of 75.9%. The 72 h period shows that films containing 5% of nanoparticles present cell viability results with a significant difference (greater than 100%) concerning the rest of the films, which have cellular viabilities less than 100% but greater than 70%. It is observed a decrease in viability between both periods of time,

however, no film, at any period of study, showed cytotoxic effect as demonstrated by the percentage of viability obtained according to ISO 10993-5, which establishes that, if viability is reduced by less than 70% of the control, a cytotoxic material is available. This can be attributed to the reaction between the cell membrane (negatively charged) and the positive charges of the functional groups present on the surface of the films (amino groups present in the main chain of chitosan) as well as the fact that nanoparticles were embedded in the polymer matrix. It is considered that the materials induce cell viability, since, in a short period of evaluation, the viability did not drop drastically as expected, and therefore are considered non-cytotoxic materials. The previous results show a relationship between the percentage of cellular viability, concentration of nanoparticles (present in the films) and exposure times, with a higher concentration of nanoparticles, longer exposure times, and lower percentages of cell viability.

Figure 6. Cell viability analysis of the films.

The count of *S. aureus* in the control and in the samples of ham treated with the films were evaluated during 4 days of storage, where the control samples (not treated with the films) showed a bacterial growth after 24 hours of the inoculation and at 96 hours they already showed bacterial growth of the order of 6 logarithmic cycles (table 4).

Table 4. Count of S. aureus after 94 h.

Samples	Log 10 CFU after 94 h of inoculation
Control	6.62
3%	3.25
7%	0.00

On the other hand, samples that were coated with films containing 3% nanoparticles show microbial growth at 96 h of storage, showing a reduction of 3 logarithmic cycles, with respect to the control. While the samples coated with films containing 7% showed no microbial development at 96 hours of the study period. This can be attributed to the reaction of the Zn^{2+} ions with the interior cellular compounds once they penetrate the cell wall of the microorganisms, as well as the oxidant agent H_2O_2 (which damages the cellular membrane of the cells produced by the surface of the ZnO nanoparticles. Also, to the antimicrobial activity of chitosan through the effect of the forces between protonated electrostatic NH_3^+ groups and the electronegative charges of the microbial surface cell. Results show lower levels of the minimum infective dose allowed (10^4) of *S. aureus* and evidence of a bacteriostatic effect of the films, agreeing with that reported by other researchers [22]. Literature pointed out that the combination of chitosan with nanoparticles and conductive polymers have provided a sensitive determination of the

analytes regarding their high surface area and high electron transfer. Also, chitosan has proven its efficiency to be employed as an immobilization platform for biomolecules using covalent, electrostatic, or entrapment approaches [23].

Conclusion

Biodegradable films reinforced with ZnO nanoparticles with thicknesses between 136 and 151 μm were developed by the casting method achieving a homogenous nanoparticle distribution and embedded in the polymer matrix with a topography of the irregular surface. The incorporation of ZnO nanoparticles to the chitosan/starch films significantly influences the mechanical properties of the film, increasing with the addition of the ZnO nanoparticles. The FTIR analysis confirmed interactions between the nanoparticles and the polymer matrix a displacement of wavenumber was detected. The nanoparticles increased the hydrophobicity and reduced the WVP of the films, a larger quantity of nanoparticles results in increased hydrophobicity. The films showed no cytotoxicity at 72 h in mouse fibroblasts. Films were effective at controlling the bacterial growth in sliced ham. According to the multifunctional properties of the films composed of chitosan/starch reinforced with ZnO nanoparticles, these have a potential as a packing material, even as a secure (GRAS) material for use in commercial food packaging.

References

1. M. Pelino, C. Cantalini, F. Veglio, Crystallization of glasses obtained by recycling goethite industrial wastes to produce glass-ceramic materials. *J. Mater. Sci.* 29 (1994) 2087-2094. https://doi.org/10.1007/BF01154684.

2. R. Barashev, S.V. Karelov, S.V. Mamyachenkov, O.S. Anisimova, Status of the organized recycling of cadmium-bearing secondary raw materials. *Metallurgist.* 57 (2013) 244-246. https://doi.org/10.1007/s11015-013-9719-8.

3. R. Bhat, N. Abdullah, R.H. Din, G.S. Tay, Producing novel sago starch based food packaging films by incorporating lignin isolated from oil palm black liquor waste. *J. Food Eng.* 119 (2013) 707–713.

4. L. Valencia-Gómez, S. Martel-Estrada, C. Vargas-Requena, J. Rivera-Armenta, N. Alba-Baena, C. Rodríguez-González, I. Olivas-Armendáriz, Chitosan/Mimosa tenuiflora films as potential cellular patch for skin regeneration. *Int. J. Biol. Macromol.* 93 (2016) 1217-1225. https://doi.org/10.1016/j.ijbiomac.2016.09.083.

5. S. A. Martel-Estrada, I. Olivas-Armendáriz, C.A. Martínez-Pérez, J.G. Chacón-Nava, Bioactividad in vitro de materiales compuestos de quitosana/poli (dl-láctido). *Rev. Mex. Ing. Quim.* 11(3) (2012) 505-512.

6. P. Kampeerapappun, D. Aht-ong, Pentrakoon, K. Srikulkit, Preparation of cassava starch/montmorillonite composite film. Carbohydr Polym 67 (2007) 155–163. https://doi.org/10.1016/j.carbpol.2006.05.012.

7. Jiménez, M.J. Fabra, P. Talens, A. Chiralt, Edible and Biodegradable Starch Films: A Review. *Food Bioprocess Technol* 5 (2012) 2058–2076. https://doi.org/10.1007/s11947-012-0835-4

8. V. Sadashiv, P. Ravindra, S. Dyawanapelly, A. Deshpande, R. Jain, P. Dandekara, Starch based nanofibrous scaffolds for wound healing applications. *Bioact. Mater.* 3(3) (2018) 255–266. https://doi.org/10.1016/j.bioactmat.2017.11.006.

9. Marra, C. Silvestre, D. Duraccio, S. Cimmino, Polylactic acid/zinc oxide biocomposite films for food packaging application. *Int. J. Biol. Macromol.* 88 (2016) 254–262. https://doi.org/10.1016/j.ijbiomac.2016.03.0390141-8130

10. C. Díaz, I. Olivas-Armendariz, J.F. Hernández Paz, C. Gómez-Esparza, H. Reyes-Blas, M. Hernández-González, C.A. Rodríguez-González, Synthesis by sol-gel and cytotoxicity of zinc oxide nanoparticles using wasted alkaline batteries. *Dig. J. Nanomater Biostructures* 12 (2017) 371-379.

11. M. Ejaz, Y.A. Arfat, M. Mulla, J. Ahmed Zinc oxide nanorods/clove essential oil incorporated Type B gelatin composite films and its applicability for shrimp packaging. *Food Packag Shelf Life* 15 (2018) 113–121. https://doi.org/10.1016/j.fpsl.2017.12.004.

12. P.J. Perez, D. Ferreira, J. dos Reis, N. José de Andrade, R. Souza, E.A. Alves, Zinc Oxide Nanoparticles: Synthesis, Antimicrobial Activity, and Food Packaging Applications. *Food Bioprocess Tech* 5 (2012) 1447-1464. doi.org/10.1007/s11947-012-0797-6.

13. F. Ferella, I. De Michelis, F. Veglio, Process for the recycling of alkaline and zinc–carbon spent batteries. *J Power Sources* 183(2) (2008) 805-811. https://doi.org/0.1016/j.jpowsour.2008.05.043

14. D. Lourdin, G. Della Valle, P. Colonna, Influence of amylose content on starch films and foams. *Carbohydr. Polym.* 27(4) (1995) 261-270. doi.org/10.1016/0144-8617(95)00071-2.

15. C. Leites, J. Menegotto, N. Zagonel, L. Kelin, L. Damaris, J. Corralo, I. Cristina, Effect of chitosan addition on the properties of films prepared with corn and cassava starches. *Int. J. Food. Sci. Tech.* 55(8) (2018) (2018) 2963–2973. https://doi.org/10.1007/s13197-018-3214-y

16. Zimoch-Korzycka,A. Rouilly, A. Bobak, A. Jarmoluk, M. Korzycki, Chitosan and cystatin/lysozyme preparation as protective edible films components. *Int. J. Polym. Sci.* 1 (2015) 1–10. https://doi.org/10.1155/2015/139617.

17. M. J.Bof, V. Bordagaray, D.E. Locaso , M.A.García, Chitosan molecular weight effect on starch-composite film properties. *Food Hydrocoll.* 51 (2015) 281-294. https://doi.org/10.1016/j.foodhyd.2015.05.018.

18. X. Zhang, G. Xiao, Y. Wang, Y. Zhao, H. Su, T. TanState, Preparation of chitosan-TiO2 composite film with efficient antimicrobial activities under visible light for food packaging applications. *Carbohydr Polym* 169 (2017) 101–107.

19. K. Saral Sarojini, M. Indumathi, G. Rajarajeswari, Mahua oil - based Polyurethane / Chitosan/ Nano ZnO composite films for biodegradable food packaging applications 124 (2019) 163-174. https://doi.org/10.1016/j.ijbiomac.2018.11.195.

20. G. Yew, A. Mohd Yusof, Z. Mohd Ishak, U. Ishiaku, Water absorption and enzymatic degradation of poly(lactic acid)/rice starch composites. *Polym. Degrad. Stabil* 90 (2005) 488e500. https://doi.org/10.1016/j.polymdegradstab.2005.04.006.

21. R.Queiroz, S. Machado, T. Haas, S. Hickmann , A. de Oliveira, Active biodegradable cassava starch films incorporated lycopene nanocapsules. *IndCrops Prod*. 109 (2017) 818–827.

22. H. Thippareddi, R. Phebus, J. Marsden, M. Singh, Antimrobial activity of Cetypyridinium chloride against Listeria monocytogenes in. ready to eat meats [disseration], Kansas State University, Manhattan 68(9) (2005) 1823-1830. https://doi.org/10.4315/0362-028X-68.9.1823

23. A. Karrat, A. Amine, Recent advances in chitosan-based electrochemical sensors and biosensors, *Arab. J. Chem. Environ. Res.* 7 (2020) 66-93

(2020) ; http://www.jmaterenvironsci.com